




Isolation enhancement of metamaterial structure MIMO antenna for WiMAX/WLAN/ITU band applications

cambridge.org/mrf

Pasumarthi Suneetha¹ , Kethavathu Srinivasa Naik¹ 
and Pachiyannan Muthusamy² 

Research Paper

Cite this article: Suneetha P, Naik KS, Muthusamy P (2022). Isolation enhancement of metamaterial structure MIMO antenna for WiMAX/WLAN/ITU band applications. *International Journal of Microwave and Wireless Technologies* **14**, 1315–1325. <https://doi.org/10.1017/S1759078721001719>

Received: 6 June 2021

Revised: 6 December 2021

Accepted: 8 December 2021

First published online: 6 January 2022

Keywords:

DG; DGS; ECC; metamaterial unit cell; MIMO antenna

Author for correspondence:

Pasumarthi Suneetha,

E-mail: rsss4m@gmail.com

¹Department of Electronics and Communication Engineering, Advanced Antenna Design Laboratory, Vignan's Institute of Information Technology (A), Visakhapatnam, Andhra Pradesh, India and ²Department of Electronics and Communication Engineering, Advanced RF Microwave & Wireless Communication Laboratory, Vignan's Foundation for Science Technology and Research (Deemed to be University), Guntur, Andhra Pradesh, India

Abstract

The μ -negative metamaterial (MNG) two-element MIMO antenna design was proposed in this article for WiMAX (2.5–2.8 GHz), WLAN (3.2–5.9 GHz), and ITU band (8.15–8.25 GHz) applications. The first design of the MIMO antenna operates at 2.7 and 4.9 GHz frequencies. In order to reduce the mutual coupling, a defective ground structure is used. For further isolation improvement, an MNG unit cell is placed in between the two radiating elements at a distance of 10 mm. The designed antenna elements have better than -23 dB coupling isolation between the two radiating elements. Moreover, with MNG an additional frequency of 8.2 GHz is obtained, which is useful for ITU band applications. The proposed antenna bandwidth is expanded by 19% in the lower operational band, 20% in the second operational band, and 32% in the higher frequency band with the MNG unit cell. From the analysis, the proposed antenna is suitable for WiMAX/WLAN/ITU band applications because of its low enveloped correlation coefficient, and highest directive gain and low mutual coupling between the radiating components. The proposed antenna was simulated, fabricated, and measured with the help of the Schwarz ZVL vector network analyzer and anechoic chamber. Both measured and simulated results are highly accurate and highly recommended for WiMAX/WLAN/ITU bands.

Introduction

Multiple MIMO antennas (Multiple Input Multiple Output) are one of the powerful ways to optimize WLAN capability. High insulation of the antenna components between them is the main obstacle for MIMO antenna architecture in order to improve device efficiency without having to include a new spectrum and extra power. Designers also suggested different structures to limit the effects of correlation between antenna components, for the application of electromagnetic band gap (EBG), defective ground structure (DGS) designs, and metamaterial unit cells. The metamaterial is a man-made device that can control the direction of electromagnetic signals. Negative refractive, reverse wave transmission, wave absorption, surface wave minimization, wave polarization, and compact architecture allow this commonplace in engineering applications such as a 3D super lens design [1, 2]. In [3] for decreasing the antenna's dimensions, two-metamaterial 2×2 MIMO antennas, composed of composite left-handed transmission lines, are designed. For isolation improvement, a DGS is used. In [4] compact modified Composite Right/Left-Handed (CRLH) 2×2 antenna is designed and for isolation improvement DGS is used. In [5] metamaterial MIMO antenna is designed without using decoupling structure for isolation improvement. In [6] ultra-wideband (UWB) MIMO antenna is designed and for high isolation frequency-selective surface is used. In [7] a new MIMO antenna architecture uses DGS to integrate Wi-Fi and Wi-Fi in UWB [8]. In the coplanar linear polarization microstrip antenna series, the periodic DGS was planned to minimize reciprocal couplings between antennas. In [9] EBG, the reciprocal connection in the X-band area patch-antenna is reduced by the EBG structure. In [10] 4×4 MIMO antenna was designed, and a DGS structure was implemented for WLAN applications to improve isolation. In [11] a structural metamaterial decoupling is designed for the improvement of the MIMO separation array of two antenna patch components, operating at 5.3 GHz. In [12] the arrangement of metamaterials is intended to decrease the mutual interaction of antenna elements of the narrow microstrip. Two elements with multiple inputs and multiple outputs (MIMO) were indeed positioned equally with a 7 mm edge-to-edge separation. By retaining the metamaterial structure between the MIMO components, the isolation rate was increased by 9 dB. In [13] meander line structure is used for better isolation between the radiating elements. In [14] a novel fractal of the

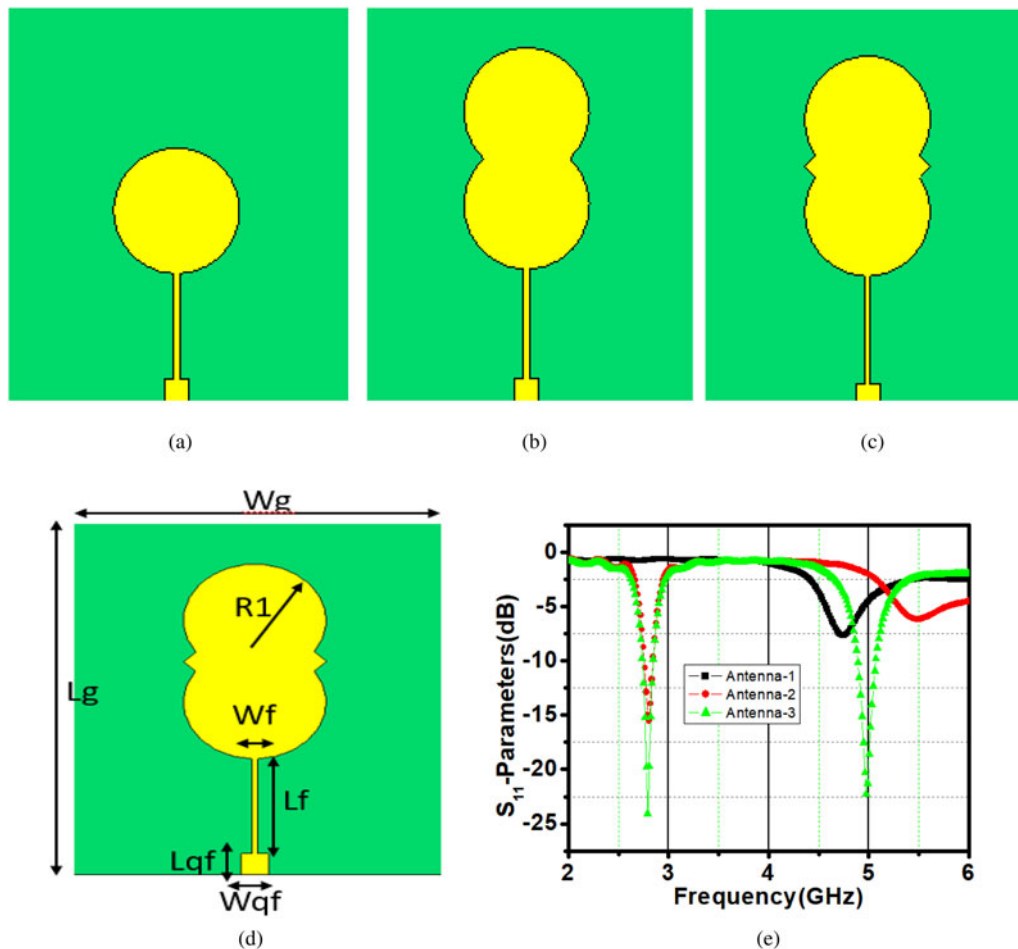


Fig. 1. Proposed single-element antenna. (a) Antenna 1; (b) antenna 2; (c) antenna 3; (d) proposed antenna; (e) S-parameter result of all the antennas.

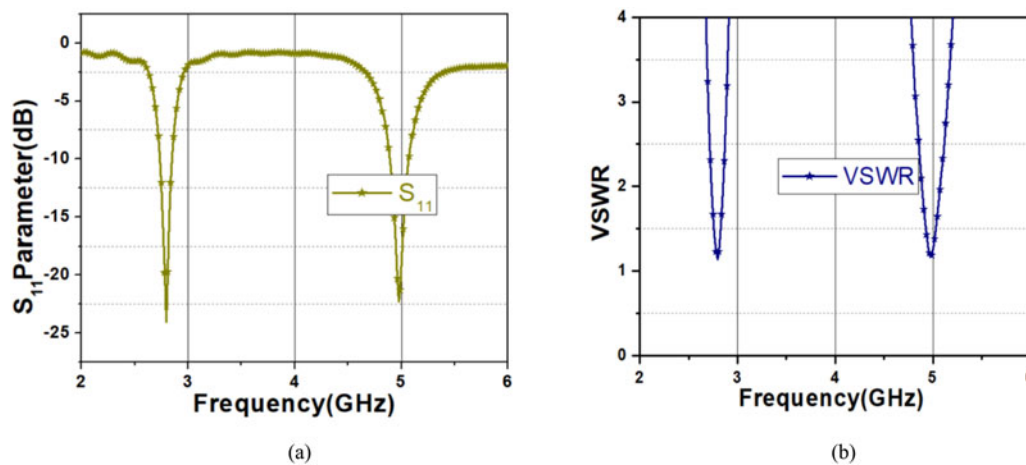


Fig. 2. Proposed single-element (a) S_{11} parameter result; (b) VSWR result.

EBG-based MIMO antenna is designed for better isolation improvement. In [15] slotted ring EBG structure is used for reducing mutual coupling between antenna 1 and antenna 2. The developed antenna is a novel metamaterial-inspired superstrate framework that can be located over a two-element MIMO antenna to increase gain, and the elements are closely

separated between them [16]. In [17] a metamaterial structure is suggested that reduces, in two elements of the MIMO network, the inevitable mutual interconnection between antennas. In [18], the loaded patch elements used in a MIMO antenna device are increased by insulation between Complementary Split-Ring Resonator (CSRR). The technique was focused on an Split Ring

Table 1. Dimensions of the proposed single-element antenna

Parameter	Wg	Lg	Wf	Lf	Wqf	Lqf	$R1$
Dimensions (mm)	40	44	0.1	13.48	3.3	5	8

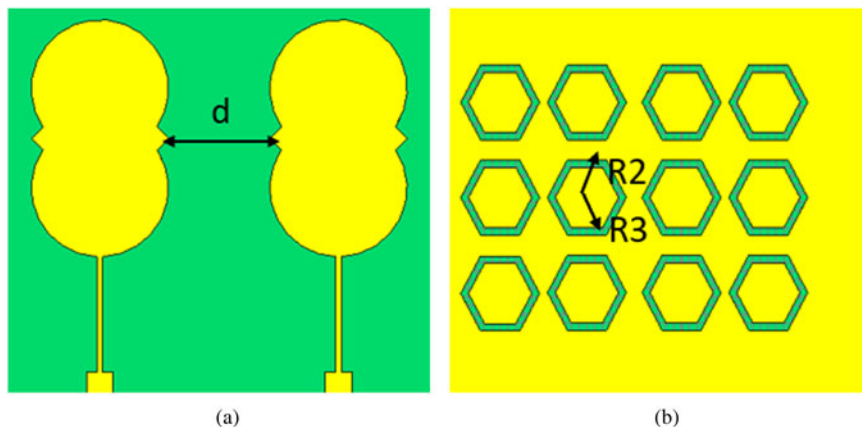


Fig. 3. (a) Front view configuration of the 1×2 MIMO antenna (b) back view.

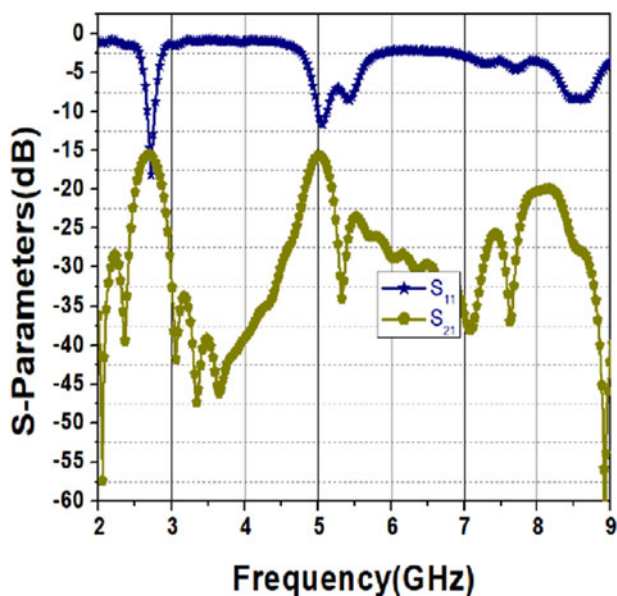


Fig. 4. Reflection coefficient result of the MIMO antenna.

Resonator (SRR) between the elements of the antenna. The insulation between antenna components has thus been increased [19] in the study. An upgraded LTE and WLAN isolation was equipped with a dual-band MIMO antenna system. The electromagnetic coupling between the proposed antennas is effectively suppressed by the double-band μ -negative metamaterial (MNG). In [20] mutual coupling reduction reduced using the neutralization and metamaterial unit-cell 20 dB isolation is improved. In [21] a review is presented on 5 G multi-element/port antenna design for wireless applications. The motivation of this work is to provide a MIMO device with a high level of insulation by not affecting other antenna performances. In [22] the authors used a three-

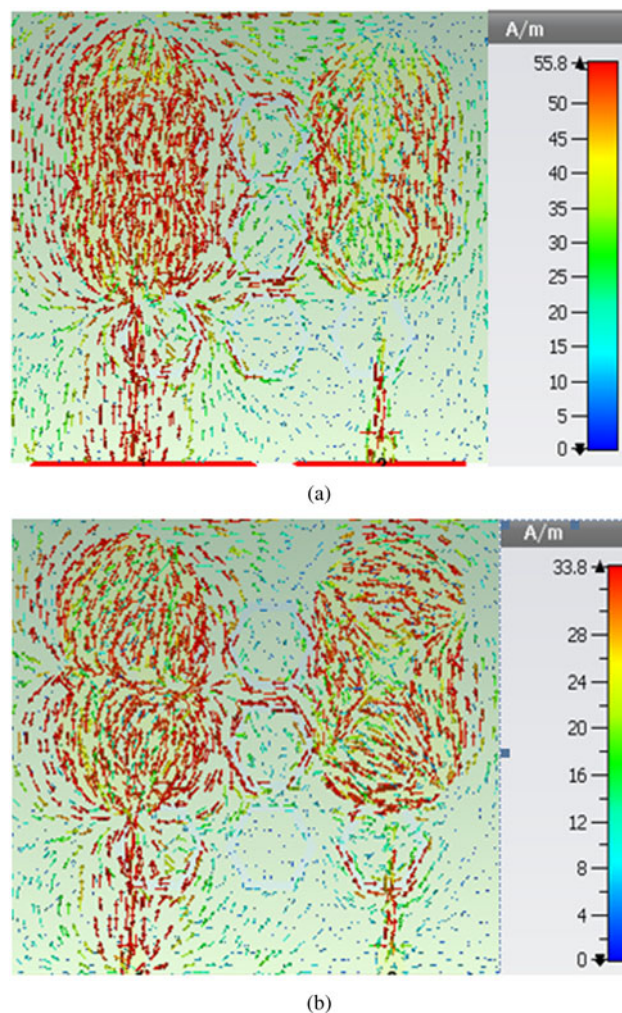


Fig. 5. Surface current distribution of the MIMO antenna. (a) 2.7 GHz; (b) 5.2 GHz.

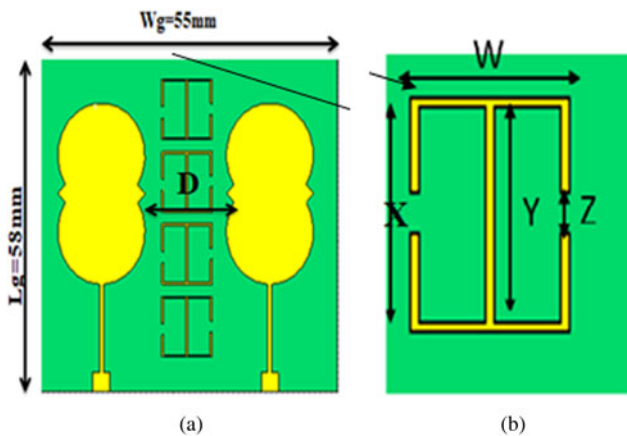


Fig. 6. Proposed metamaterial-based MIMO antenna. (a) Front view; (b) unit cell.

Table 2. Dimensions of the proposed metamaterial unit cell

Parameter	Dimensions (mm)
D	10
W	3
X	3
Y	2.8
Z	0.3

dimensional metamaterial structure (3DMMS) to decrease mutual coupling in a two-element patch antenna array. The 3DMMS is made up of two shorted pins which connect an upper M-shaped patch and two lower U-shaped patches. In [23] to minimize undesired mutual coupling between antenna components, a multi-layered EBG (ML-EBG) structure was integrated into a MIMO antenna. An enhanced EBG and three loading patches with the same distance make up the proposed ML-EBG structure. In [24] a dual-band eight-antenna array for 5G mobile terminals MIMO applications was proposed. Eight L-shaped slot antennas based on stepped impedance resonators comprise up the designed MIMO antenna array Surface Insulation Resistance (SIRs). In [25] to decrease the mutual coupling between two tightly dipole antennas to maintain cross-polarization suppression, a ceramic superstrate-based decoupling technique was developed. In [26] high isolation was achieved by incorporating a novel wheel-like meta-material structure into the closely placed antenna elements of a small broadband antenna array with two identical antenna elements. To decrease coupling from adjacent antenna components, a wheel-like meta-material decoupling structure is placed between the two antenna elements. In [27] a dual-band MIMO was designed for Wi-MAX/WLAN applications. T-shaped junctions, which function as a short stub loaded resonator, are utilized for high isolation. In [28] an array of 7×7 double-negative metamaterial unit cell was utilized to improve the gain, bandwidth, and low mutual coupling. In [29] a lattice of 2×5 unit cells of meta-material design is used to improve the gain, bandwidth, and also for low mutual coupling of the antenna. Based on the above literature work, in this proposed research work, we introduced 3×4 a hexagonal-shaped DGS and MNG unit cell is placed on top layer between radiating elements with a distance of 10 mm. This is to improve isolation and reduce mutual coupling between the

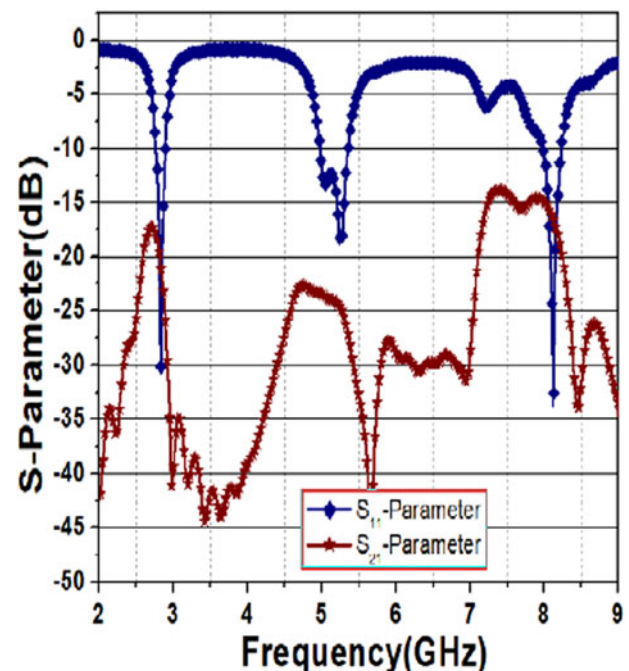


Fig. 7. S_{11} and S_{21} metamaterial-based MIMO antenna.

radiating elements. The existing antenna resonates at single and dual band frequencies with high isolation, whereas its isolation is 23 dB with a multiband operated antenna. The detailed dimensions and resonant frequency of proposed antenna are compared with existing antenna as reported in this paper. A portable antenna for WiMAX, WLAN, and ITU is planned for operation within this paper. The architecture and analysis of the framework are based on the 2018 CSTMW. The prototype with an optimized structure for metamaterial is generated and the effects are simulated by measured results as regards the reflective coefficient.

Antenna design 1

The proposed single-element antenna is constructed with low-cost FR4 substrate material with a thickness of 1.6 mm, a loss tangent value of 0.02, and a relative permittivity of 4.3. The proposed work was initially designed for 4.8 GHz by using a conventional circular micro-strip patch antenna with a radius of 8 mm. Later, another circular shape was attached with a conventional antenna-like doublet shape, and finally a triangular shape was inserted in the middle of both edges to attain the dual-band resonant frequency of 2.7 and 4.9 GHz. Figures 1(a)–1(e) show the step-by-step design of the proposed antenna and S-parameter results. Figure 2(b) shows the VSWR result which satisfied the < 2 (Table 1).

Design of 1×2 MIMO antenna 2

In this session, two similar antennas are used to design a 1×2 MIMO antenna. The antennas are separated by a 12 mm distance. The overall dimension of the desired MIMO antenna is $55 \text{ mm} \times 51 \text{ mm} \times 1.6 \text{ mm}$. The desired MIMO antenna is shown in Fig. 3(a). For better isolation, partial ground is introduced which shows the back view of Fig. 3(b). The dimensions of the inner and outer ring hexagonal circle are 5 and 4 mm, respectively; DGS low

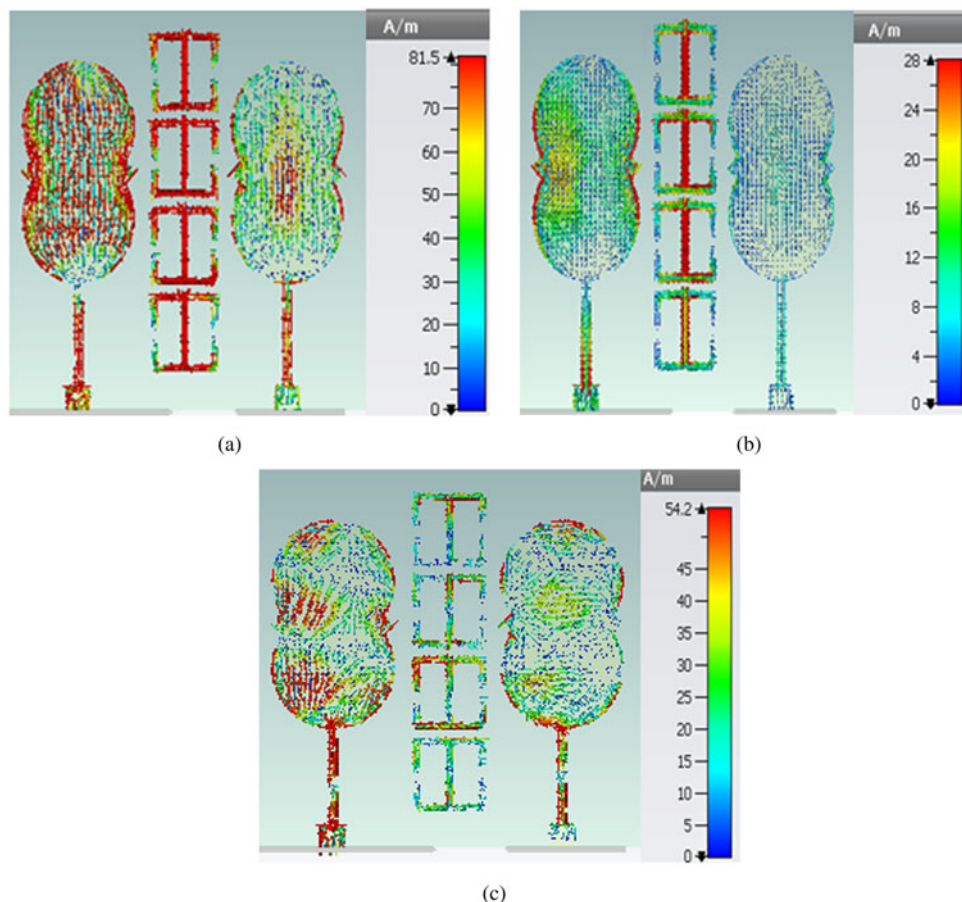


Fig. 8. Surface current distribution at (a) 2.7 GHz; (b) 5.2 GHz; and (c) 8.2 GHz.

improvement of bandwidth is achieved and the transmission coefficients are also not < -20 dB. Figure 4 shows the simulated performance of the original MIMO antenna reflection coefficients (without metamaterial unit cell). Figure 5 shows the surface current distribution at 2.7 and 5.2 GHz. When one port is activated, the current density on the non-excited antenna element is extremely high, resulting in significant mutual coupling between the two radiating components.

Design of metamaterial MIMO antenna 3

In “Antenna design 1” section, the mutual coupling increases due to the low distance between the patch antennas but as the separation between the two elements is increased the mutual coupling can be reduced. But without increasing the distance, the MNG unit cell is placed in between the radiating elements; this leads to reduced mutual coupling. Due to the introduction of MNG, an 8.2 GHz frequency band was additionally obtained, which is used for ITU band applications. Figure 6(a) shows a metamaterial-based MIMO antenna, Fig. 6(b) shows the MNG unit-cell structure, and Table 2 shows the dimensions of the proposed metamaterial unit cell.

In this proposed design due to the unit-cell structure, the center frequency is shifted from 4.9 to 5.2 GHz, which is useful for WLAN applications. The unit cell is designed for a 2.7 GHz operating frequency. Figure 7 shows the S_{11} and S_{21} results of

the three bands metamaterial MIMO antenna. At 2.7 GHz, S_{11} and S_{21} are -30 and 18.35 dB, respectively; at middle frequency, S_{11} is -18.99 dB and S_{21} is -23.32 dB; and at 8.2 GHz, S_{11} is -34.43 dB and S_{21} is -17.75 dB. By the observation, the center frequency band achieved good isolation other than two band frequencies. Figures 8(a)–8(c) show the surface current distribution at 2.7, 5.2, and 8.2 GHz. At 2.7 GHz, we observe that majority of the current flow in the metamaterial unit cell in comparison to second radiating element as a result of minimal mutual coupling is obtained. At 5.2 GHz, maximum current flow in the metamaterial unit cell and no current flow in the second radiating element result in extremely low mutual coupling. At 8.2 GHz, the majority of the current flows in the metamaterial unit cell compared to the second radiating element result in low mutual coupling.

Other important antenna parameters such as antenna radiation pattern, gain, and antenna efficiency are determined for appropriate application. In this way, the proposed antenna analysis with the help of the anechoic chamber measured and simulated the results of E and H plane radiation pattern, gain, and efficiency, which is shown in Figs 9 and 10, and Table 3 reported the comparison of simulated and measured values. By observing this radiation pattern, the results are nearly omnidirectional pattern which means they are uniform in all the plane directions. This kind of pattern is recommended for Wi-MAX/WLAN/ITU bands.

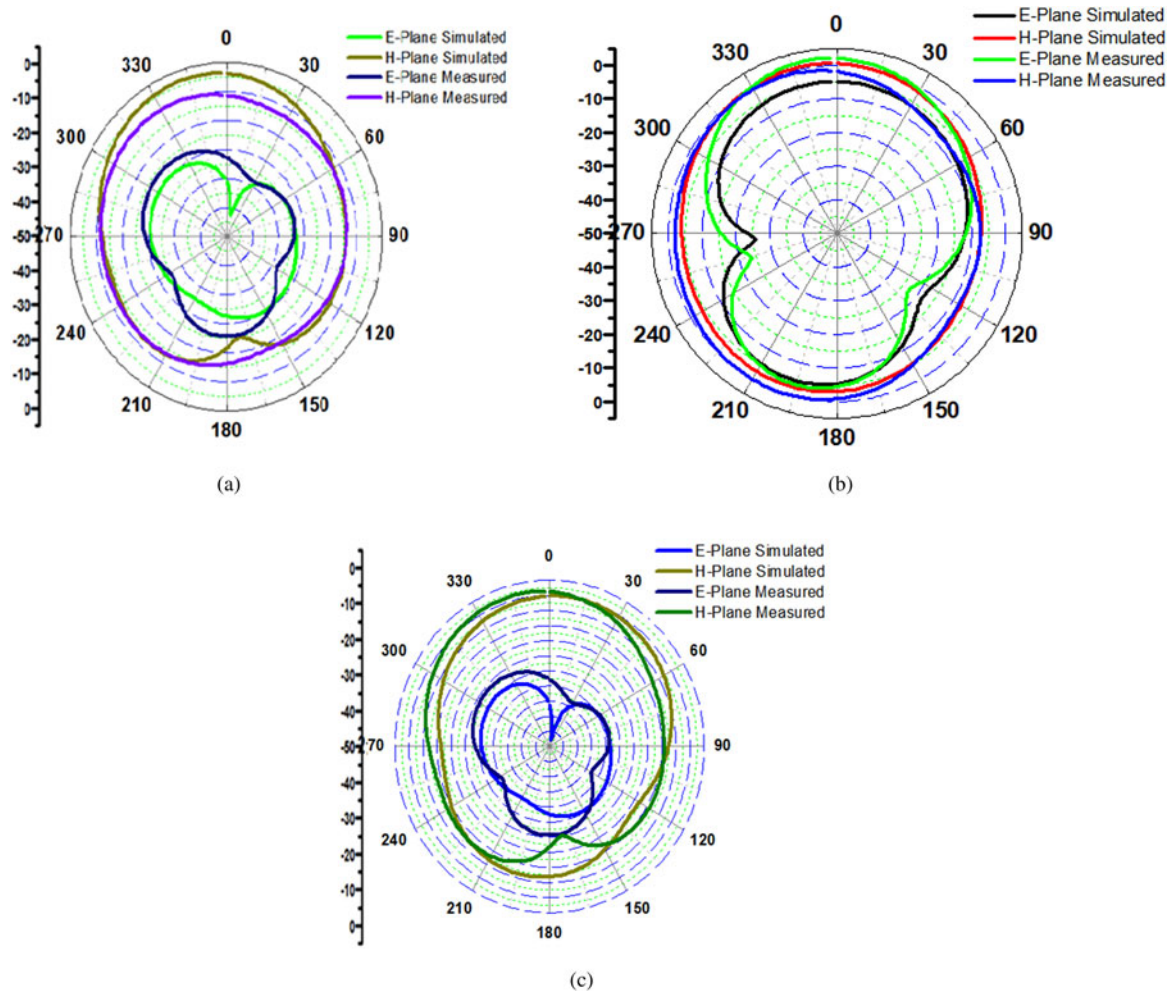


Fig. 9. Radiation pattern at (a) 2.7 GHz; (b) 5.2 GHz; and (c) 8.2 GHz.

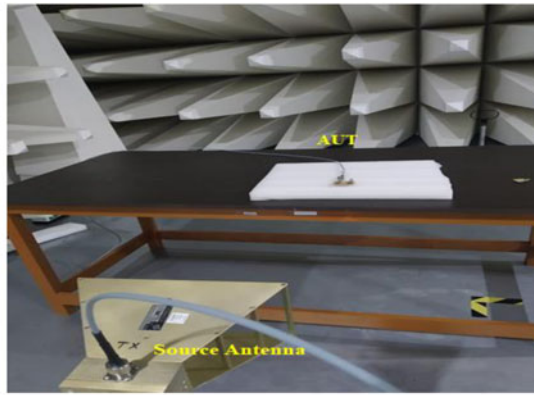
The measured and simulated 3D radiation patterns at frequencies of 2.7, 5.2, and 8.2 GHz of the designed MIMO antenna are shown in Fig. 9. The measurement is carried out by using a Schwarz ZVL vector network analyzer and a double ridge guide horn antenna setup inside the anechoic chamber. The anechoic chamber is used to get perfect measurement data, which significantly reduces the external effect of soundings. Figure 10 shows the photograph of the antenna under test for obtaining the radiation pattern, gain, and radiation efficiency. According to the findings, the measured and simulated results are in excellent agreement with the proposed MIMO antenna at 2.7 and 8.2 GHz which produce a quasi-omnidirectional radiation pattern, and 5.2 GHz produces an omnidirectional pattern. The simulated and measured antenna radiation efficiency average value is 85% in the operational frequency bands. At the desired frequency bands, the gain of the simulated and measured antenna is nearly identical. Figure 11 shows the performance analysis parameters of the enveloped correlation coefficient (ECC) and directive gain (DG). At the operational frequencies, the proposed MIMO antenna has a simulated ECC of <0.01, whereas the DG is 9.998 magnitude. Figure 12 shows the front view and back

view of the prototype antenna, and Fig. 13 shows the simulated and measured results of the proposed antenna. Table 4 shows a comparison table for various MIMO antennas with existing work.

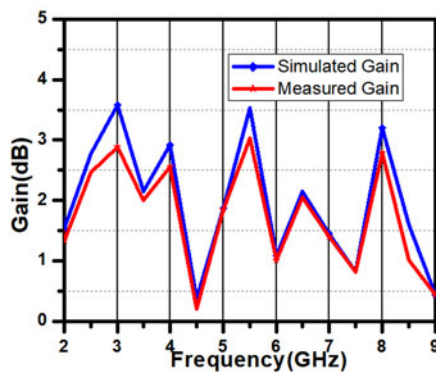
MIMO antenna characteristics

The efficiency of MIMO antennas in terms of diversity must be measured. The ECC is a measurement of the correlation between radiation elements. The ECC's low value provides high isolation between antennas. Radiation variations or scattering parameters may be used to quantify the factor. The enveloped correlation, which is simply the square of the correlation coefficient, can be determined easily and rapidly from S-parameters for a basic two-port network in a standardized multipath environment. ECC can be calculated using equation (1).

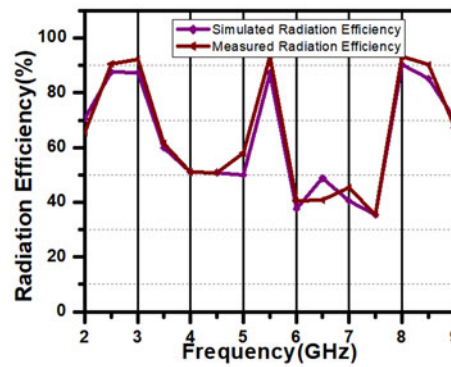
$$\rho_{eij} = \frac{|S_{ii}^* S_{ij} + S_{ji}^* S_{jj}|^2}{(1 - |S_{ii}|^2 - S_{ij}^2)(1 - |S_{jj}|^2 - S_{ij}^2)} \quad (1)$$



(a)



(b)



(c)

Fig. 10. The photographs of antenna under measurement for (a) radiation pattern; (b) gain; (c) radiation efficiency.

Table 3. Proposed antenna simulated and measured results

Characteristics	Simulated frequency in GHz			Measured frequency in GHz		
	2.7	5.2	8.2	2.7	5.2	8.2
S_{11} (dB)	-30.12	-18.99	-34.43	-22.53	-17.65	-33.89
S_{21} (dB)	-18.35	-23.32	-17.75	-18.55	-23.32	-17.75
Gain (dB)	3.1	2.8	2.6	3	2.7	2.8
% of Radiation Efficiency	84	83	85	85	84	86

Directive gain

DG measures the transmission power loss for the MIMO systems. The DG could be measured using equation (2).

$$DG = 10\sqrt{1 - |\rho_{eij}|^2}. \tag{2}$$

Metamaterial unit-cell configuration to minimize mutual coupling

The desired metamaterial structure exhibits the property of negative permeability. The antenna is printed on FR4 substrate material with a thickness of 1.6 mm, a dielectric constant value of 4.3, and 0.02

loss tangent $\tan(\delta)$. The characteristics of the metamaterial unit cell are analyzed with the help of S_{11} and S_{21} which is reported in Fig. 14(a). It shows that the phase difference is 180 degrees and proves that it satisfies the basic characteristics. The effective real and imaginary part of metamaterial unit cell is in Fig. 14(b). It proves the negative permeability characteristics of the metamaterial unit cell. Figures 14(c) and 14(d) show the simulation set up with boundary conditions and a two-port representation of the unit cell.

Parametric study of metamaterial unit cell

In this section, the parametric analysis was carried out in order to evaluate the performance of MIMO system and response of one unit-cell and two unit-cell S-parameter is shown in Fig. 15(a).

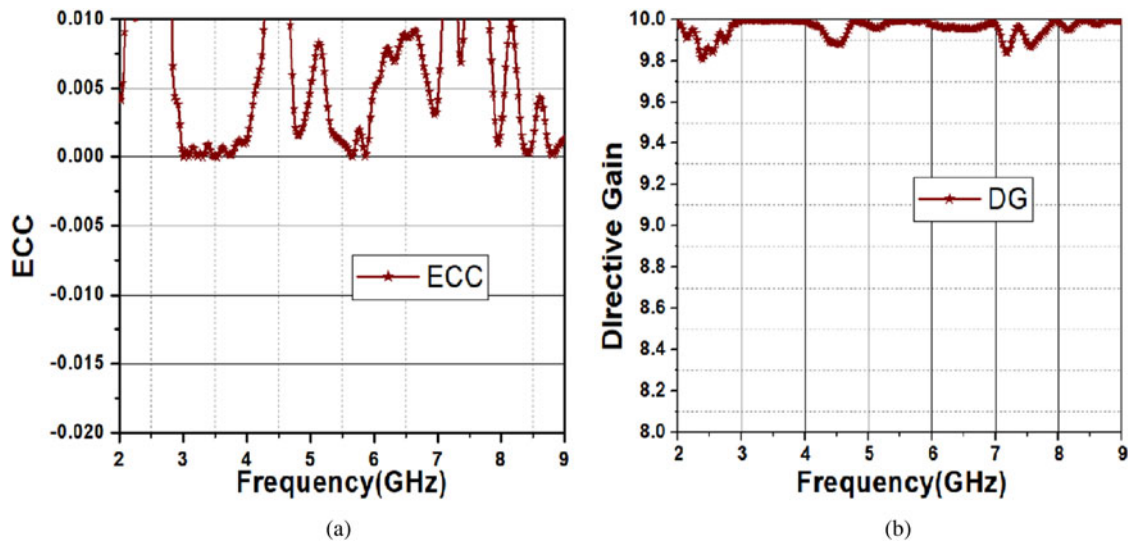


Fig. 11. MIMO characteristics plot (a) ECC; (b) DG.

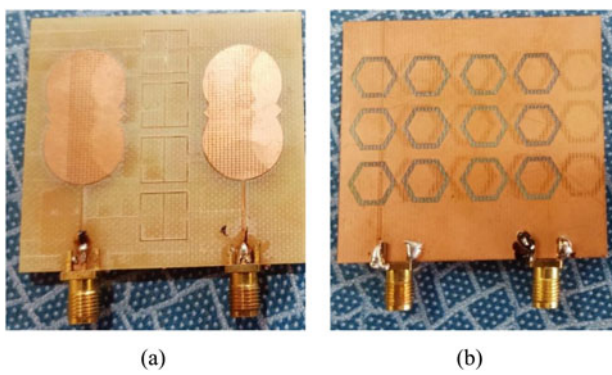


Fig. 12. Prototype antenna (a) front view and (b) back view.

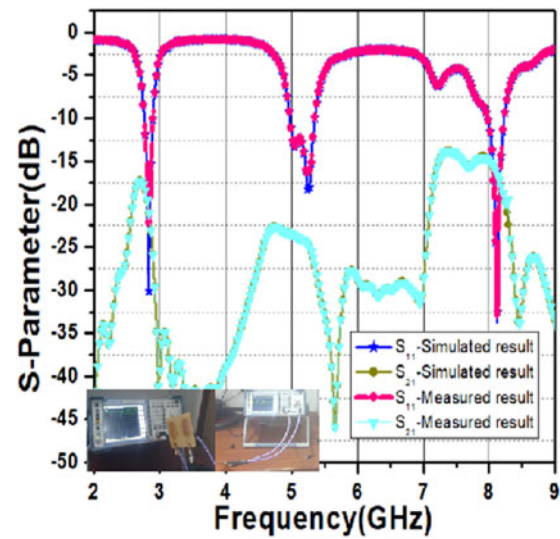


Fig. 13. Proposed antenna measured and simulated results.

Table 4. Comparison table for various MIMO antennas with existing work

Reference Antenna	Dimensions (mm)	No of elements	Isolation (dB)	ECC	DG	Frequency
5	29 × 26 mm ²	2	10	0.0002	–	5.8 GHz
9	40 × 40 mm ²	2	Not given	–	–	10.2 GHz
11	40 × 30 mm ²	2	12.5	–	–	5.3 GHz
17	52.3 × 128 mm ²	2	5	–	–	2.4 GHz
22	60 × 60 mm ²	2	18	–	–	2.35 GHz
23	28.3 × 15.5 mm ²	2	30	–	–	2.55 GHz
24	140 × 70 × mm ²	8	11.8	<0.1	–	(3400–3600 MHz) and (5150–5925 MHz)
25	100 × 100 mm ²	2	30	0.4	–	3.5 GHz
26	26 × 18 mm ²	2	20	0.10	–	X-band
27	38 × 36 × mm ²	2	19	9.81/9.98	0.16	2.5/5.8 GHz
28	107 × 58 mm ²	4 × 2	41	–	<0.0006	5.2–6.4
29	137 × 77 mm ²	4	18	–	<0.02	5.8 GHz
Proposed work	55 × 51 mm ²	2	5	0.0002	9.999	2.8/5.2/8.2 GHz

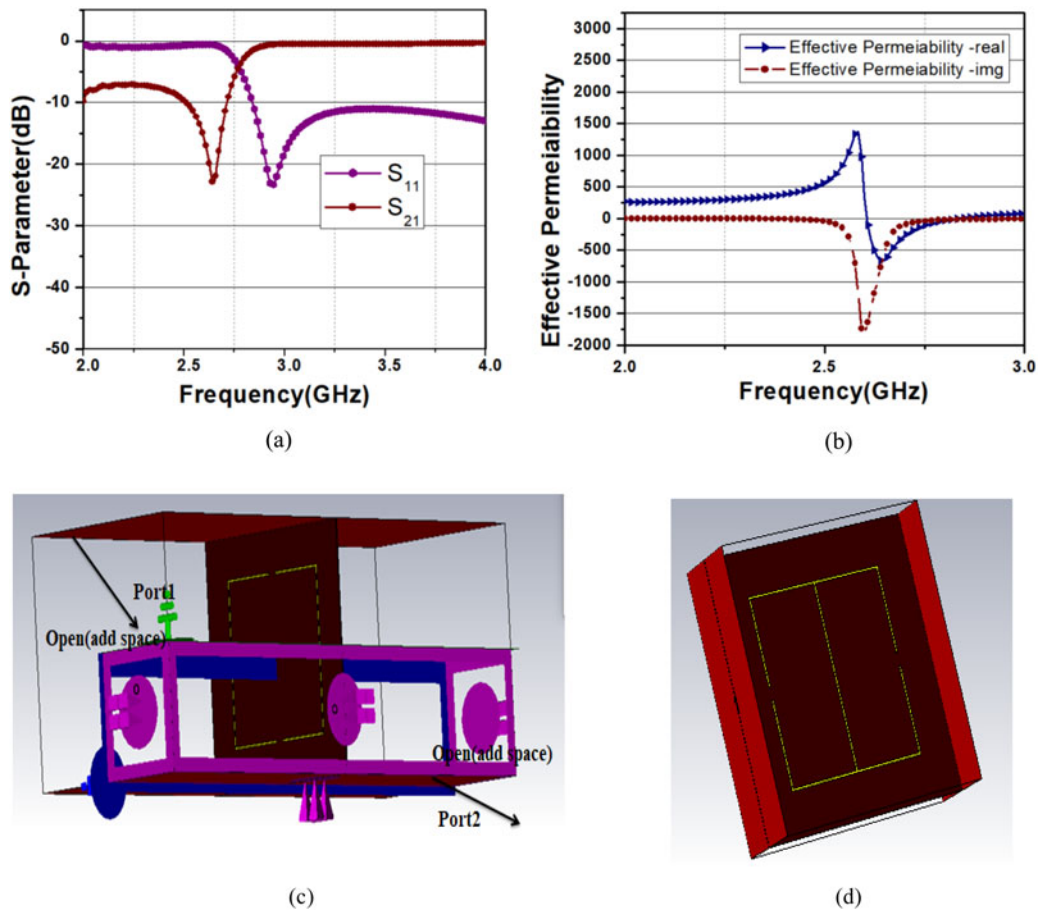


Fig. 14. Unit-cell characteristics plot: (a) S-parameters; (b) effective permeability; (c) simulation set up of the unit cell; (d) two-port representation of unit cell.

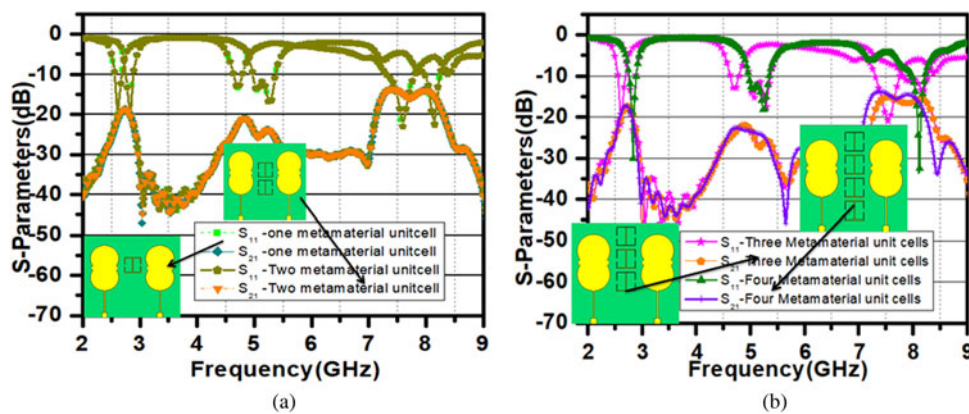


Fig. 15. S-parameter result: (a) one and two unit cells; (b) three and four unit cells.

The single unit cell is introduced between radiating elements. Later, two unit cells are placed. By observing the return loss value of both one and two unit cells, which is similar, an additional frequency of 8.2 GHz was also obtained because of

indirect coupling of the metamaterial unit cells. However, the return loss value is not an acceptable value for frequencies of 2.7 and 5.2 GHz. In order to make further improvements, three and four unit cells are arranged and analyzed. The

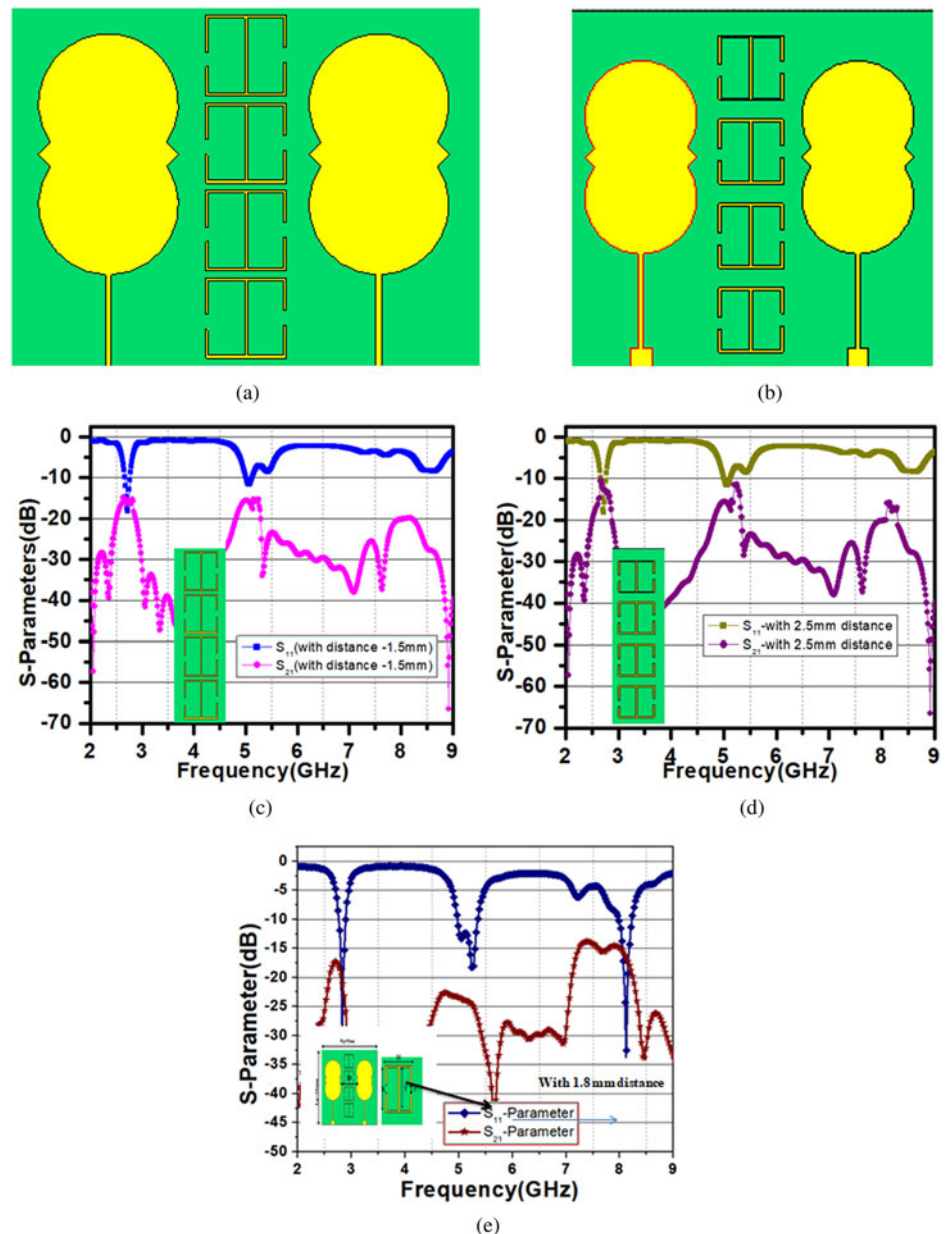


Fig. 16. Distance between metamaterial unit cells: (a) 1.5 mm; (b) 2.5 mm; (c) S-parameter of the 1.5 mm; (d) S-parameter of the 2.5 mm; (e) S-parameter of the 1.8 mm.

return loss results of the three and four unit cells are shown in Fig. 15(b) and it has shown extremely good impedance matching.

The distance between each unit cell is taken at 1.8 mm to obtain good isolation and lower return loss values. The analysis is carried out at a distance of 2.5, 1.5, and 1.8 mm. The return loss results are shown in Fig. 16. It observed that the distances of 2.5 and 1.5 mm unit cells exhibited low return loss and low isolation values when compared to the proposed antenna with a distance of 1.8 mm.

Conclusion

The present study proposes a 1×2 MIMO MNG for reducing the mutual coupling of tightly packed radiating elements. In comparison to previous studies, the suggested technique provides superior isolation between antennas. At 2.7, 5.2, and 8.2 GHz, the isolation values are 17.85, 24.35, and 15.45 dB, respectively. In summary, the antenna may be recommended

for use in WIMAX, WLAN, and ITU operational frequency bands.

Acknowledgement. This work is supported by DST science and engineering research board (SERB) with file no: EEQ/2016/000391.

References

- Xu HX, Wang GM and Li MQ (2013) Three-dimensional super lens composed of fractal left-handed materials. *Advanced Optical Materials* **1**, 495–502.
- Xu HX, Wang GM, and Qi MQ (2013) Metamaterial lens made of fully printed resonant-type negative refractive index transmission lines. *Applied Physics Letters* **102**, 193502.
- Phuong HNB, Hie QN and Chien DN (2015) Novel metamaterial MIMO antenna with high isolation for WLAN applications. *International Journal of Antennas and Propagation* **2015**, 1–9. doi: <https://doi.org/10.1155/2015/851904>.

4. **Torabia Y, Bahrib A and Sharifib A-R** (2015) A novel metamaterial MIMO antenna with improved isolation and compact size based on LSRR resonator. *IETE Journal of Research* **2015**, 1–9. doi: <http://dx.doi.org/10.1080/03772063.2015.1085335>.
5. **Ibrahim A, Abdalla MA and Shubair RM** (2017) High-isolation metamaterial MIMO antenna 978-1-5386-3284-0/17/\$31.00, IEEE. doi: 10.1109/APUSNCURSINRSM.2017.8072911
6. **Zhu X, Yang X and Lui QSB** (2017) Compact UWB-MIMO antenna with metamaterial FSS decoupling structure in EURASIP. *Journal on Wireless Communications and Networking* **2017**, 1–6.
7. **Rao TV, Alapati S and Raju K** (2018) Novel technique of MIMO antenna design for UWB applications using defective ground structures. *Materials Science Journal of Scientific & Industrial Research* **7**, 66–69.
8. **Wei K, Li J-Y, Wang L, Xing Z-J and Xu R** (2016) Mutual coupling reduction of microstrip antenna array by periodic defected ground structures. *IEEE 5th Asia-Pacific Conference on Antennas and Propagation (APCAP)*. doi: 10.1109/APCAP.2016.7843257.9
9. **Kumar N** (2017) To reduce mutual coupling in microstrip patch antenna arrays elements using electromagnetic band gap structures for X-band, 978-1-5090-5913-3/17/\$31.00 c. IEEE. doi: 10.1109/ICNETS2.2017.8067937
10. **Santhi M and Robinson S** (2021) Design and analysis of 4x4 MIMO antenna with DGS for WLAN applications. *International Journal of Microwave and Wireless Technologies* **13**, 979–985. doi: <https://doi.org/10.1017/S1759078720001658>.
11. **Luo S and Li Y** (2018) MIMO antenna array decoupling based on a metamaterial structure, 978-1-5386-5648-8/18/\$31.00 c 2018. IEEE. doi: 10.1109/APCAP.2018.8538027
12. **Iqbal A, Saraereh OA, Bouazizi A and Basir A** (2018) Metamaterial-based highly isolated MIMO antenna for portable wireless applications. *Electronics* **7**, 1–8. doi: 10.3390/electronics7100267.
13. **Ghosh J, Ghosal S, Mitra D and Chaudhuri SRB** (2016) Mutual coupling reduction between closely placed microstrip patch antenna using meander line. *Progress in Electromagnetics Research Letters* **59**, 115–122.
14. **Naderi M, Zarrabi FB, Jafari FS and Ebrahimi S** (2018) Fractal EBG structure for shielding and reducing the mutual coupling in microstrip patch antenna array. *AEUE*, 52386. <https://doi.org/10.1016/j.aeue.2018.06.028>.
15. **Attia H and Sheikh SI** (2019) Microstrip antenna array with reduced mutual coupling using slotted-ring EBG structure for 5 G applications, 978-1-7281-0692-2/19/\$31.00 ©2019. IEEE. doi: 10.1109/APUSNCURSINRSM.2019.8889318
16. **Mark R, Rajak N, Mandal K and Das S** (2019) Metamaterial based superstrate towards the isolation and gain enhancement of MIMO antenna for WLAN application. *International Journal of Electronics and Communications (AEÜ)*, 1434–8411. <https://doi.org/10.1016/j.aeue.2019.01.011>.
17. **Khan U and Sharawi MS** (2014) Isolation improvement using an MTM inspired structure with a patch based MIMO antenna system, 978-88-907018-4-9/14/\$31.00. IEEE.
18. **Abdelhamid C, Marwa D, Sakli H and Hamrouni C** (2019) High isolation with metamaterial improvement in a compact UWB MIMO multi-antennas, 978-1-7281-1820-8/19/\$31.00 ©2019. IEEE.
19. **Tu T, Van Hoc N, Son PD and Van Yem V** (2017) Design and implementation of dual-band MIMO antenna with low mutual coupling using electromagnetic band gap structures for portable equipments. *International Journal of Engineering and Technology Innovation* **7**, 48–60.
20. **Abdelhamid C and Sakli H** (2020) Mutual reduction in the coupling of the MIMO antenna network applied to the broadband transmission. *Advances in Science, Technology and Engineering Systems Journal* **5**, 338–343. doi: 10.25046/aj050244
21. **Gupta P, Malviya L and Charhate SV** (2019) 5 G multi-element/port antenna design for wireless applications. *International Journal of Wireless Technology* **11**, 918–938. doi: 10.1017/s1759078719000382.
22. **Hwangbo S, Yang HY and Yoon Y-K** (2016) Mutual coupling reduction using micromachined complementary meander line slots for a patch array antenna. *IEEE Antennas and Wireless Propagation Letters* **16**, 16671670. doi: 10.1109/LAWP.2017.2663114.
23. **Jiang T, Jiao T and Li Y** (2018) A low mutual coupling MIMO antenna using periodic multi-layered electromagnetic band gap structures. *ACES Journal* **33**, 305–311.
24. **Li J, Zhang X, Wang Z, Chen X, Chen J, Li Y and Zhang A** (2017) Dual-band eight-antenna array design for MIMO applications in 5 G mobile terminals. *IEEE Access* **7**, 71636–71644.
25. **Liu F, Guo J, Zhao L, Huang GL, Li Y and Yin Y** (2020) Ceramic superstrate-based decoupling method for two closely packed antennas with cross-polarization suppression. *IEEE Transactions on Antennas and Propagation* **68**, 1–6. doi: 10.1109/TAP.2020.3016388.
26. **Jiang J, Xia Y and Li Y** (2019) High isolated X-band MIMO array using novel wheel-like metamaterial decoupling structure. *ACES Journal* **34**(19), 1829–1836.
27. **Dkiouak A, Zakriti A, El Ouahabi M and Mchbal A** (2019) Design of two element Wi-MAX/WLAN MIMO antenna with improved isolation using short stub loaded resonator (SSLR). *Journal of Electromagnetic Waves and Applications* **34**, 1268–1282. doi: 10.1080/09205071.2020.17569927
28. **Ojo R, Jamlos MF, Soh PJ, Jamlos MA, Bahari N, Lee YS, Al-Bawri SS, Karim MSA and Khairi KA** (2020) A triangular MIMO array antenna with a double negative metamaterial superstrate to enhance bandwidth and gain. *Wiley Periodicals LLC* **30**, 1–12. doi: 10.1017/S175907871900059X.
29. **Lan N and Van Yem V** (2019) Gain enhancement for MIMO antenna using metamaterial structure. *International Journal of Microwave and Wireless Technologies* **11**, 851–862.



Pasumarthi Suneetha is working as an Assistant Professor in Vignan's Institute of Information Technology(A), Visakhapatnam, India. She received her B.Tech. degree in 2008 from JNTU Kakinada, the M.Tech. degree in 2013 from JNTU Kakinada. She is pursuing the Ph.D. degree from VFSTR University, Guntur, AP, India. Her areas of interest are MIMO antennas and wireless communications. She published 10 publications in reputed inter-

national journals and conferences.



K. Srinivasa Naik has received his Bachelor of Engineering in Electronics and Communication Engineering, Master of Engineering, and Ph.D. degrees from Andhra University. At present, he is working as an Associate Professor in the Department of Electronics and Communication Engineering, Vignan's Institute of Information Technology (A), Duvvada, Visakhapatnam. He has presented more than 40 technical papers in reputed journals. He completed One DST project worth 50 lakhs. He is a life member of SEMCE (I). His research interests include array antennas, EMI/EMC, communications, field theory, and instrumentation.



Pachiyanan Muthusamy received the Ph.D. degree in Information and Communication Engineering in the area of UWB antenna at Anna University, Chennai, India. He is currently working toward the DGS structure-based UWB antenna for WBAN applications and object detection. He has 12 years of both academic and industrial experience and has published several international journal and conference papers. He is currently working as an Associate Professor in the ECE department at Vignan's Foundation for Science, Technology & Research. He is working on antenna compactness using DRA and meta materials. His research area includes UWB antennas, coplanar waveguides, meta materials, DRA, and RF circuits.